Metal−Support Interactions in Zeolite-Supported Noble Metals: Influence of Metal Crystallites on the Support Acidity

David Kubička,[†] Narendra Kumar,[†] Tapani Venäläinen,[‡] Hannu Karhu,[§] Iva Kubičková,[†] Heidi Österholm,[||] and Dmitry Yu. Murzin*[,†]

Laboratory of Industrial Chemistry, Process Chemistry Centre, Åbo Akademi University, Biskopsgatan 8, FIN-20500 Åbo/Turku, Finland, Department of Chemistry, University of Joensuu, P.O. Box 120, FIN-08101 Joensuu, Finland, Department of Physics, University of Turku, Vesilinnantie 5 20014, Turku, Finland, and Neste Oil Oy, POB 310, FIN-06101 Porvoo, Finland

Received: October 10, 2005; In Final Form: January 25, 2006

The metal−support interactions on a series of catalysts of different acidities, including platinum-modified zeolites and H−MCM-41, are investigated by means of XPS, CO and pyridine adsorption, and a model reaction (ring opening of decalin). The electronic properties of Pt are influenced by the acidity of the support, and the alteration of Pt properties increases with increasing acidity of the support, as can be seen from the changes in the Pt binding energy and stretching frequency of adsorbed CO. At the same time, the presence of platinum affects the acidic properties of the supports by reducing the strength of the acid sites. This is observed directly as the changes in desorption of pyridine from the acid sites and indirectly as the suppression of cracking reactions during the ring opening of decalin on the Pt-modified catalysts. The observed results are discussed in terms of the interatomic potential model.

1. Introduction

Metal modification of zeolites provides a possibility for preparing catalysts with unique properties.[1−8] The presence of Brønsted acid sites and metal clusters in zeolite pores makes the zeolites bifunctional, i.e., it enables catalytic transformations that require both metal and acid active sites. Typical examples of the use of bifunctional catalysis are the hydroisomerization of *n*-alkanes and hydrocracking.[9−11] In addition to opening a new reaction pathway for the isomerization and cracking of saturated hydrocarbons, the metal improves the catalytic stability of the acidic zeolites by suppressing the formation of carbonaceous deposits blocking the zeolite pores and acid sites.[12,13]

The conceivable effect of steric constraints on the morphology of zeolite-supported metals and thus on their catalytic properties is accompanied by another far more intriguing phenomenon—the change in the electronic properties of the supported metals. Ever since the first report on the electron deficiency of a platinum cluster supported on an acidic support,[14] the investigation of this fundamental issue has attracted constant attention from many researchers. Advanced physicochemical characterization techniques are essential to study the interactions between metal clusters and their supports and to elucidate the relationship between the observed changes in the reaction rates of numerous catalytic reactions and these interactions. The rapid development of spectroscopic methods in recent years has brought a deeper understanding of the effects of the support on the morphology and electronic properties of supported metal clusters.[15] The shifts to lower frequency in the infrared spectra of CO adsorbed on supported metals correlate with the increasing support alkalinity and are attributable to the changes in the electron density of the supported metal.[16−21] Moreover, the shifts in the binding energy of supported metal clusters determined by XPS indicate that metal clusters supported on acidic supports are electron deficient[19,22,23] and that their electron deficiency increases with increasing concentration of acid sites.[23]

The explanations that have been put forward to account for the changes in the catalytic activities and electronic properties of supported metal clusters include the formation of metal−proton adducts;[3,4,24,25] polarization of the metal crystallites by neighboring cations;[26] charge transfer between the metal atoms and zeolite oxygen atoms;[16] and most recently, a shift in the ionization potential of valence orbital electrons together with charge rearrangement from the particle to or from the metal−support interface.[20,27−29] The proton−metal adduct model was described primarily for Pd supported in zeolite Y[24,25] and was extended to other metals including Rh,[3] Ru, and Au.[15] Moreover, it is not capable of explaining the increase in electron density on metal clusters in alkaline zeolites.[27] Nevertheless, there is strong evidence for the interaction between the protons in zeolite Y and supported Pd clusters.[25] The model proposed by Mojet et al.[20,27] relies on the results of new spectroscopic techniques (atomic XAFS and Pt−H shape resonance) combined with catalytic data for the conversion of neopentane. It is further supported by the traditional spectroscopic methods (FTIR spectroscopy of adsorbed CO, XPS), EXAFS, and theoretical calculations.[29] The EXAFS results indicate that metal atoms (Pt, Pd) are in direct contact only with the support oxygen atoms.[20] The authors infer that the change in electron charge of the support oxygen atoms, which is determined by the Madelung potential of the support, causes a change in the interatomic potential of the Pt atoms. This was followed by the change in the intensity of the Fourier transform AXAFS peak, and the

* To whom correspondence should be addressed, Laboratory of Industrial Chemistry, Process Chemistry Centre, Åbo Akademi University, FIN-20500 Åbo/Turku, Finland. Tel.: +358 2 215 4985. Fax: +358 2 215 4479. E-mail: dmurzin@abo.fi.

[†] Åbo Akademi University.

[‡] University of Joensuu.

[§] University of Turku.

[||] Neste Oil Oy.

10.1021/jp055754k CCC: $33.50
Published on Web 02/24/2006

metal−support interaction was attributed to a change in the energy position of the metal valence d orbitals interacting with adsorbates.[20,27,29] By combining these results with ab initio calculations on a Pt_4O_3 cluster and molecular orbital calculations, they proposed that the metal−support interaction induces a charge rearrangement from the particle to or from the metal−support interface.[29] This model excludes[27] a charge transfer from the metal to the support with increasing charge on the oxygen atoms proposed previously.[16]

A vast majority of the investigations of metal−support interactions focus solely on the alteration of the morphology[15,30] or electronic properties[3,16,20,27,29] of the metal by the support. It can be expected, however, that the Madelung potential of the support will be affected by the supported metal clusters. In fact, it has been mentioned previously[3] that the interaction between the acid and metal active sites was mutual, but investigations of the influence of the metal on the acidic properties of the support are scarce.[31−33] The present study focuses on the description of the mutual modification of acid sites and supported metal active sites in metal-modified zeolites and mesoporous materials. It shows that the changes in the electronic properties of Pt supported on a series of supports with varying acidities are accompanied by changes in the distribution of the acid site strengths. In addition to the results obtained by spectroscopic methods (XPS, FTIR spectroscopy), the mutual modification of both types of active sites, i.e., metal and acid sites, is supported by the changes in the product distributions in the ring opening of decalin.[34,35]

2. Experimental Section

2.1. Catalyst Preparation. H−Beta-75 (CP811E-75), NH_4-Beta-25 (CP814E), and NH_4-Mordenite (CBV21A) zeolites were obtained from Zeolyst International. The ammonium-form zeolites were transformed into the corresponding proton forms through a step calcination procedure at 773 K in a muffle oven. Na−MCM-41 mesoporous molecular sieve was synthesized according to published procedures[36,37] with some modifications,[38] and it was transformed to NH_4-MCM-41 by an ion-exchange method using ammonium chloride solution. The subsequent step calcination at 773 K in a muffle oven produced H−MCM-41. The determination of the structure and phase purity of Na−MCM-41 mesoporous molecular sieve was carried by X-ray powder diffraction (Philips PW 1800). SiO_2 was purchased from Merck.

The prepared proton-form catalysts and silica were impregnated with a solution of hexachloroplatinic acid to obtain a loading of platinum on the catalysts equal to 2 wt %. The impregnation procedure was accomplished by drying of the impregnated catalysts at 383 K. It was confirmed by X-ray diffraction that the zeolite and H−MCM-41 structures were not affected by the impregnation. The dried catalysts were directly reduced at 623 K in a flow of hydrogen prior to characterization and catalytic experiments. It was reported previously that platinum-containing species originating from impregnation with hexachloroplatinic acid are readily reduced to metallic platinum at 570 K.[39] Moreover, the XPS data do not reveal the presence of Pt^{2+} or Pt^{4+} in the reduced samples. For one of the catalysts (Pt/H−Beta-25), a procedure involving calcination at 723 K followed by reduction at 623 K was investigated, and the experimental and characterization results were compared to those of directly reduced Pt/H−Beta-25.

2.2. Catalyst Characterization. The chemical compositions of the investigated materials, in terms of Si/Al ratios, are reported in Table 1. The residual content of Na cations expressed as Na_2O was 0.05 wt %.[40] Marques et al. have reported the total and framework Si/Al ratios of NH_4-Beta-25 (CP814E) to be 12.5 and 15.5, respectively.[41] The specific surface areas of the proton-form catalysts and their corresponding Pt-impregnated counterparts were measured by the nitrogen adsorption method (Sorptometer 1900, Carlo Erba Instruments). The catalysts were outgassed at 473 K prior to the measurements, and the Dubinin and BET equation were used to calculate the specific surface areas of the zeolites and H−MCM-41 and SiO_2, respectively.

TABLE 1: General Physical Properties of the Studied Catalysts

	Si/Al	metal loading, wt %	specific surface area, m^2/g	
modification[a]	H, Pt	Pt	H	Pt
H−Mordenite	10	2	605[b]	584[b]
H−Beta-25	12.5	2	807[b]	752[b]
H−Beta-75	37.5	2	664[b]	−
H−MCM-41	20	2	1242[c]	992[c]
SiO_2	−	2	379[c]	−

[a] H denotes original catalysts; Pt denotes catalysts impregnated with Pt. [b] Calculated by the Dubinin equation. [c] Calculated by the BET equation.

A Perkin-Elmer PHI 5400 ESCA apparatus was used for the X-ray photoelectron spectroscopy (XPS) analysis of the platinum-modified catalysts. Monochromatized Al Kα radiation with an energy of 1486.6 eV and sensitivity factors of 4.798, 0.283, and 3.354 for Cu 2p, Si 2p, and Zn $2p_{3/2}$, respectively, was used. The catalysts were reduced ex situ under flowing hydrogen at 623 K for 2 h, with a heating and cooling rate of 5 K/min. The reduced catalysts were mounted on two-sided tape and transferred to the XPS system under N_2 atmosphere. A pass energy of 17.9 eV was used. A flood gun was used to stabilize the surface for electric charging under X-ray radiation. The silicon 2p photoelectron line 103.3 eV[42] was used to correct the binding energy axis for electric charging. Spectral background caused by inelastically scattered photoelectrons was removed using Shirley's method. A Voigt-like mixture of Gaussian and Lorentzian line shapes was used in the line fitting procedure. The precision of the observed binding energy values is ±0.2 eV. Because the Pt $4f_{7/2}$ line was visible, an energy separation of 3.33 eV[42] and a 4:3 intensity ratio were routinely used as constraints in line fitting to deconvolute the strongly overlapping Pt $4f_{5/2}$ and Al 2p photoelectron lines. Sensitivity factors for Pt 4f, Si 2p, Al 2p, Cl 2p, and O 1s were 4.674, 0.283, 0.193, 0.770, and 0.711, respectively.

The adsorption of CO on platinum-modified catalysts was investigated by infrared spectroscopy (ATI Mattson FTIR). The catalyst samples were pressed into self-supported wafers and reduced in situ in an FTIR cell in flowing hydrogen (AGA, 99.999%) at 623 K for 2 h. The reduction was completed by evacuation for 30 min at the reduction temperature. The reduced catalysts were then cooled to room temperature (298 K), and the spectral background was measured. In the course of the actual measurements, the catalysts were first contacted for 30 min with flowing gas containing 10% CO in He. Following a short evacuation (5−10 min) at 298 K, the spectra of adsorbed CO on Pt supported on the studied catalysts were collected. The shift in the position of the linearly bound CO (2070−2090 cm^{-1}) was used to evaluate the interaction between Pt and the support. All spectra were recorded with a spectral resolution equal to 2 cm^{-1}. The ratio of the linearly bound CO to the bridge-bound CO (1700−1900 cm^{-1}) indicated the adsorption stoichiometry of CO on Pt, and the areas of the peaks, which

correspond to the amount of surface Pt atoms, were compared with the results obtained by dispersion measurements.

Metal dispersion of the catalysts was determined from the amount of chemisorbed CO measured using a pulse method. The experiments were carried out using a Micromeritics TPD/TPR 2910 AutoChem instrument. A sample (100−150 mg) was set in the quartz U-tube and reduced in a H_2 stream (AGA, 99.999%, 20 mL/min). A ramp rate of 5 K/min was applied, and the temperature was linearly raised to the final temperature 623 K, where it was held for 120 min. Then, the specimen was cooled to 313 K under flowing He (AGA, 99.9999%), and when the baseline was stable, the experiment was started. The CO (AGA, 99.997%) pulse was repeated until the adsorption was saturated. The calculation of the dispersion based on the cumulated amount of carbon monoxide assumed the stoichiometry of CO to platinum to be unity, as confirmed by the FTIR measurements.

Hydrogen temperature-programmed desorption (H_2 TPD) was performed for Pt/H−Beta zeolites using a Micromeritics TPD/TPR 2910 AutoChem instrument. The catalysts (ca. 0.15 g) were reduced in flowing hydrogen (AGA, 99.999%) at 623 K for 2 h, cooled to ambient temperature, and flushed with He (50 mL/min, AGA, 99.9999%) for 1 h before the experiments were started. Hydrogen was desorbed by heating the samples at a rate of 5 or 10 K/min to 823 K in flowing He (50 mL/min). The samples were kept at 823 K for 30 min before the experiments were completed.

The acidities of proton-form and platinum-modified catalysts were measured by infrared spectroscopy (ATI Mattson FTIR) using pyridine (≥99.5%, a.r.) as a probe molecule for qualitative and quantitative determination of both Brønsted and Lewis acid sites. The samples were pressed into thin self-supported wafers (10−12 mg/cm^2), mounted into an FTIR cell, and evacuated at 723 K for 1 h. Then, the samples were cooled to 373 K, and background spectra were measured prior to pyridine adsorption. Pyridine was first adsorbed for 30 min at 373 K and then desorbed by evacuation at different temperatures (523, 623, and 723 K) to obtain a distribution of acid site strengths. All spectra were recorded under vacuum at 373 K with a spectral resolution equal to 2 cm^{-1}. Spectral bands at 1545 and 1450 cm^{-1}, respectively, were used to identify Brønsted (BAS) and Lewis (LAS) acid sites. The amounts of BAS and LAS were calculated from the intensities of the corresponding spectral bands using the molar extinction coefficients reported by Emeis.[43]

Additionally, the total acidities of H−Beta-25 and Pt/H−Beta-25 were determined using temperature-programmed desorption of ammonia (NH_3 TPD) in an AMI-100 instrument (Altamira Instruments Zeton Inc.) equipped with a thermal conductivity detector (TCD). Dried sample (ca. 40 mg) was mounted in the sample tube; pretreated in helium flow (AGA, 99.999%) at 353 K for 20 min; and ramped to 773 K at a constant rate of 20 K/min, where it was held isothermally for 1 h. After the sample had been cooled to the adsorption temperature (473 K), ammonia (AGA, 10% NH_3 in helium) was adsorbed on it for 1 h. The sample was flushed for 1 h at 473 K with helium and cooled to 373 K in He before NH_3 desorption was started. The following TPD temperature profile was used: holding for 30 min at 373 K, heating at a constant rate of 20 K/min to 773 K, and maintaining the temperature at 773 K for 30 min.

2.3. Catalytic Experiments. Catalytic experiments using a mixture of decalin (bicyclo[4.4.0]decane) isomers (Fluka, ≥98%) with a cis-to-trans ratio of 2:3 were performed to study the effects of metal−support interactions on the activity and selectivity of the catalysts under study. One hundred milliliters of decalin and 4 g of an in situ reduced catalyst were employed in each experiment. The experiments were performed in an electrically heated 300-mL stainless steel autoclave (Parr Industries) in the presence of hydrogen (99.999%) in the kinetic regime. The reaction was carried out at a temperature of 523 K and an overall pressure of 2 MPa, which corresponds to a hydrogen partial pressure of 1.7 MPa. The liquid reaction products were analyzed with a gas chromatograph (Agilent 6890N) equipped with a capillary column (DB-Petro, 100 m × 0.2 mm × 0.5 μm) and a Flame ionization (FI) detector. GC/MS was applied to identify the reaction products. Additional details of the experimental procedures and product analysis can be found elsewhere.[34,35]

3. Results and Discussion

3.1. Influence of the Support on the Electronic Properties of Supported Pt. The alteration of the electronic properties of supported metals by the support is well documented in the literature for various supports, especially reducible oxides, such as TiO_2, and zeolites.[3,44−46] Because the present study focuses on zeolites and mesoporous aluminosilicates, only the metal−support interactions in zeolite-supported metals will be discussed here. Several models have been proposed to explain this phenomenon[3,16,20,24,26,27] Despite the different interpretations,[3,16,20,24,26,27] the experimental data supporting them are in very good agreement. Depending on the binding energy of the supported metals, observed by XPS, the wavenumber of CO adsorbed on the supported metal crystallites in FTIR spectra increases while the character of the support changes form alkaline to neutral and then acidic.[20] Moreover, the prevailing mode of adsorption of CO on the metal is also different on acidic and alkaline supports: the linearly bound CO prevails on metals on acidic supports, whereas the bridged mode of adsorption of CO is found to be important on metals on alkaline supports.[16,20,21] Recently, essential information on the metal−support interactions has been obtained from advanced analysis of XAFS spectra (AXAFS, EXAFS, XANES).[20,27−29] In addition to physical methods, several model reactions, such as hydrogenolysis of neopentane[3,20,27] and competitive hydrogenation of benzene−toluene mixtures,[47] have been exploited to shed more light on the nature of the metal−support interactions. In the present study, XPS and FTIR spectroscopy of adsorbed CO were used to investigate the interactions between platinum and its supports and to describe the influence of the acidity of the supports on the supported platinum clusters.

Some general characteristics of the investigated catalysts are listed in Table 1. Although the loadings of platinum reported in Table 1 are nominal loadings, the platinum content of 1.9 wt % in Pt/H−MCM-41, determined by the direct current plasma (DCP) method, justifies the use of the nominal values in this case, as the same procedure was employed in the preparation of all studied catalysts. Despite the small decrease in the specific surface area of the catalysts after their impregnation with platinum, which can be possibly explained by blockage of some of the micropores, the specific surface areas of the impregnated zeolites and H−MCM-41 remain very high (>580 m^2/g) (see Table 1), and it can be expected that this decrease does not significantly affect their catalytic activity. Further characterization of the proton-form zeolites can be found elsewhere.[48]

The results of the XPS analysis of the platinum-modified catalysts are summarized in Figure 1, with the corresponding numerical values of the binding energy of Pt $4f_{7/2}$ reported in Table 2. A clear shift in the binding energy (BE) of Pt $4f_{7/2}$ to

TABLE 2: Characterization of Pt-Modified Catalysts by CO Adsorption and XPS

	CO on Pt by FTIR spectroscopy		CO pulse chemisorption[a]			XPS
catalyst	position of peak maximum,[b] cm^{-1}	relative peak area	dispersion, %	relative dispersion	average crystallite size, nm	Pt binding energy,[c,d] eV
Pt/H−Mordenite	−	−	45	0.82	2.5	71.9
Pt/H−Beta-25	2081	1.00	55	1.00	2.0	71.8
Pt/H−Beta-75	2079	0.95	52	0.95	2.2	71.4
Pt/H−MCM-41	2073	1.57	73	1.33	1.6	71.4
Pt/SiO_2	−	−	27	0.49	4.2	71.2

[a] Assuming spherical Pt particles and CO/Pt stoichiometry equal to unity. [b] Accuracy = 2 cm^{-1}. [c] Pt $4f_{7/2}$. [d] Accuracy = 0.2 eV.

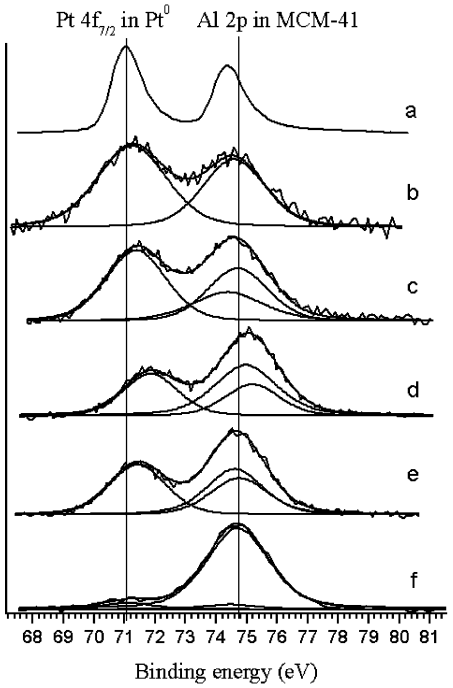

Figure 1. Deconvolutions of Pt $4f_{7/2}$, $4f_{5/2}$ doublets and Al 2p lines (where Al is present) from (a) Pt(111) single crystal, (b) $Pt-SiO_2$, (c) Pt−Beta-75, (d) Pt−Mordenite, (e) Pt−MCM-41, and (f) 0.2Pt−MCM-41, obtained from reduced catalysts with pass energy set to (a) 4.45, (b−e) 17.9, and (f) 71.55 eV.

TABLE 3: Brønsted and Lewis Acidities of Fresh Catalysts

	Brønsted acid sites, μmol/g			Lewis acid sites, μmol/g		
catalyst	523 K	623 K	723 K	523 K	623 K	723 K
H−Mordenite	331	284	212	71	50	39
H−Beta-25	269	207	120	162	128	113
H−Beta-75	147	135	114	39	29	16
H−MCM-41	26	11	3	40	20	12
SiO_2	−	−	−	−	−	−
Pt/H−Mordenite	373	183	0	61	10	0
Pt/H−Beta-25	304	178	0	163	33	0
Pt/H−Beta-75	164	46	0	55	6	0
Pt/H−MCM-41	39	9	0	95	9	0
Pt/SiO_2	0	0	0	9	0	0

higher values than found for Pt single crystals can be seen for all of the investigated catalysts except Pt/SiO_2 (see Figure 1). The shift increases with increasing acidity of the support (see Table 3). The binding energies of small particles, however, require a very careful consideration. Several factors are involved in the BE shift, and therefore, the degree of electron deficiency is difficult to evaluate quantitatively.[22] For example, the small size of metal crystallites results in a BE shift[49] that is largely due to changes in band structure and the loss of metallic character. It was shown[50] that decreasing the size of Pd

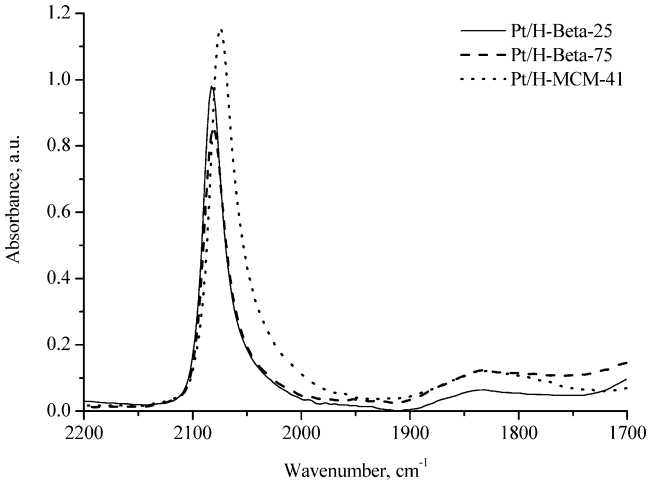

Figure 2. FTIR spectra of CO adsorbed on Pt supported on supports with different acidities. Supports: H−Beta-25 (—), H−Beta-75 (− − −), H−MCM-41 (• • •).

crystallites supported on various supports (C, SiO_2, Al_2O_3) from 4 to 1 nm results in a linear increase of the BE of Pd equal to ca. 0.6 eV. Over a narrower range of metal crystallite sizes, such as the 1 nm observed in the present study for Pt/zeolites and Pt/MCM-41, smaller variations in the metal binding energy due to changes in metal crystallite sizes can be expected, e.g., about 0.1 eV in the present case. However, a much larger difference in the BE of Pt (ca. 0.5 eV) is found in the current study, and it can be thus be attributed predominantly to the differences in the acidities of the investigated catalysts. Moreover, the apparent discrepancy where Pt in the more acidic Pt/H−Beta-75 has the same BE as in Pt/H−MCM-41 (see Table 2) can be explained by the slightly smaller size of Pt crystallites in the latter catalyst. It can therefore be inferred that the shift in the BE of Pt $4f_{7/2}$ is caused by the increasing acidity of the supports and that it reflects the interaction between the platinum and the support, as has been observed by others as well.[3,15,20,22,23]

Shifts in the CO stretching frequency have been previously reported to be caused by the changes in the electronic properties of supported metals.[16,20,22] However, it is difficult to interpret these shifts conclusively, given that they are influenced by crystallite size[51] and surface coverage[52,53] in addition to the changes in the metal electronic properties.[16,20,22,53] The transmission FTIR spectra of CO adsorbed on supported Pt crystallites are compared in Figure 2. Catalysts with rather similar Pt crystallite sizes (1.6−2.2 nm) and large differences in the concentration of the acid sites (BAS = 26−269 μmol/g) were selected for the comparison of the changes in the CO stretching frequency while suppressing the impact of the variation in the Pt crystallite sizes. As expected, a shift to higher wavenumber with increasing support acidity is observed, although it is not as pronounced as in the previous studies,[20] which covered a wider range of support acidity/alkalinity. Moreover, the FTIR band corresponding to the stretching frequency of bridge-bonded

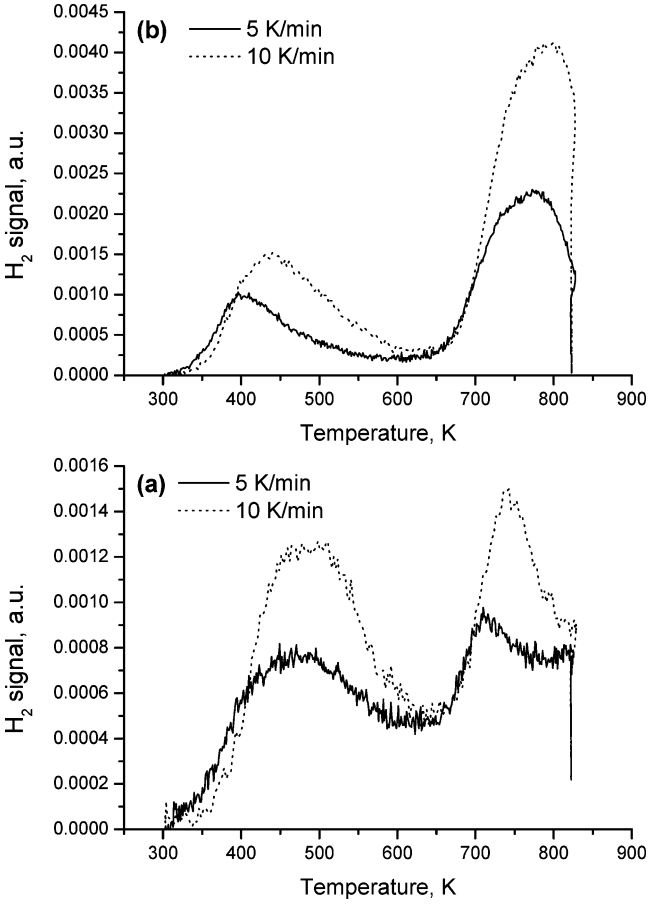

Figure 3. H_2 TPD profiles of (a) Pt/H−Beta-25 and (b) Pt/H−Beta-75.

CO is very weak, thus suggesting that a vast majority of the CO is adsorbed linearly. Consequently, the almost exclusive linear adsorption of CO on Pt clusters substantiates the assumption of the CO/metal stoichiometry being equal to unity. The area of the CO adsorption band corresponds to the number of Pt atoms exposed to CO, i.e., it is proportional to the specific surface area of the metal. The relative area of the FTIR band corresponding to linearly bonded CO, which is reported in Table 2, can be correlated with the relative dispersion of Pt on the catalysts (see Table 2) and further supports the results obtained by CO pulse chemisorption. The results of CO adsorption on supported Pt crystallites followed by FTIR spectroscopy are in agreement with the results obtained by XPS and indicate that the electronic properties of platinum are altered by the support. Moreover, the extent of this alteration is shown to depend on the acidity of the support.

Desorption of hydrogen was used to determine the effect of changes in Pt electronic properties on the chemisorption of H_2 on the Pt crystallites. The H_2 TPD profiles of Pt/H−Beta-25 and Pt/H−Beta-75 displayed multiple hydrogen desorptions (see Figure 3). Two peaks can be distinguished: the first having a desorption maximum around 430 K and the latter above 670 K (see Figure 3). They were ascribed to hydrogen chemisorbed on platinum and to spillover hydrogen, respectively.[54,55] In addition to these two peaks, a hydrogen desorption peak with a maximum around 550 K was reported[54,55] and assigned to hydrogen held between the metal particle and the support surface (interfacial hydrogen).[55] It is conceivable that this desorption peak is present in the investigated catalysts as well, but is severely overlapped with the hydrogen desorbing from platinum and therefore does not show a distinct maximum. Consistently, a rather broad desorption peak is observed in the region 373−573 K (see Figure 3). The complete overlap of the peaks corresponding to hydrogen adsorbed on platinum and on the metal−support interface hinders a reliable determination of the hydrogen desorption energy. Nevertheless, the differences in the desorption profiles of Pt/H−Beta-25, on one hand, and Pt/H−Beta-75, on the other, can still be evaluated qualitatively. Despite the overlap of the peaks, it is clear from Figure 3 that hydrogen desorbs from Pt/H−Beta-25 at higher temperatures than it desorbs from Pt/H−Beta-75. Because the Pt crystallite size is almost the same for both Pt/H−Beta zeolites (see Table 2) and they differ only in their acidities (see Table 3), the difference in the desorption profiles can be associated with the difference in the acidity. The higher temperature of the hydrogen desorption from platinum indicates that the Pt−H bond is stronger in Pt/H−Beta-25, i.e., in the more acidic catalyst. This is in agreement with the conclusions of Koningsberger et al. based on Pt−CO FTIR spectroscopy, Pt−H shape resonance, and AXAFS,[21] and it further supports the conclusions drawn here from XPS and Pt−CO FTIR spectroscopy.

3.2. Influence of the Supported Pt Crystallites on the Acidic Properties of the Support. 3.2.1. Physical Characterization Methods: Pyridine FTIR Spectroscopy and NH_3 TPD. Only minimal attention has been paid so far to the influence of the supported metal crystallites on the properties of the acidic supports.[31−33,56] The present study, however, demonstrates that, when metals are supported on zeolites, the acidic properties of the supporting zeolite are modified in addition to the modification of the electronic properties of the supported metal as discussed above. Moreover, the modification of the acidic properties might be responsible for changes in the catalytic activity and selectivity of the metal-modified zeolites as discussed below. To investigate the acidic properties of the proton-form and platinum-modified zeolites in detail, pyridine was first adsorbed on the catalysts and then desorbed at different temperatures to characterize the strengths of the acid sites. The adsorption and desorption of pyridine on the studied catalysts was followed by FTIR spectroscopy, which enables Brønsted acid sites (BAS) to be distinguished from Lewis acid sites (LAS) and their concentrations to be determined quantitatively. The results are summarized in Table 3.

A dramatic difference between the proton-form zeolites, on one hand, and the platinum-modified zeolites, on the other, is revealed upon examination of Table 3; the strongest acid sides, both BAS and LAS, observed in the proton-form zeolites disappear when the H−zeolites are impregnated with platinum. Nevertheless, the total concentration of BAS and LAS remains unchanged or increases after the introduction of Pt for all investigated catalysts (see Table 3). The concentration of the Lewis acid sites increases most likely as a result of the interaction of pyridine with platinum crystallites, given that the metal crystallites are known to be acceptors of electron pairs, i.e., to act as Lewis acids.[57,58] On the other hand, it is more difficult to account for the slight increase in the concentration of BAS in the remaining Pt-modified catalysts. Possibly, the new Brønsted acid sites are formed during the impregnation process, e.g., through ion exchange of the nonacidic cations compensating the framework charge for protons.

The virtually unchanged total concentrations of BAS and LAS after modification of zeolites with platinum and accompanied by the complete disappearance of the strongest acid sites, i.e., those that can retain pyridine at temperatures higher than 723 K, offer a sole plausible interpretation of the observations: platinum modifies the strength of the acid sites. Alternatively,

one could ascribe the observed changes in the distribution of acid sites to modification of the support during the impregnation procedure due to leaching of Al from the framework positions or removal of extraframework aluminum species given that it is known that treatment of zeolites by acids leads to their dealumination.[59] Marques et al. have recently shown[60] that extraframework Al species present in H−Beta-25 (the same catalyst as used in this study) were extracted much faster then framework aluminum in the course of treatment in 1 M HCl. At the same time, a dramatic decrease of the concentration of Lewis acid sites, determined by FTIR spectroscopy following pyridine adsorption, was observed.[60] Because no such decrease of the Lewis acidity was found in the current study, it can be concluded that both framework and extraframework aluminum species are not affected by the impregnation procedure. Furthermore, the chemical shift and the width of the Al peak in zeolite A in the ^{27}Al MAS NMR spectrum were not affected by the impregnation of the zeolite with a solution of H_2PtCl_6.[61] It can thus be inferred that the observed changes in the distribution of the acid site strengths originate from the interactions between the Pt crystallites and the support.

Current investigations of metal-modified zeolites show that the reduction of the acid site strengths is not limited only to platinum and the supports reported here; similar trends have been observed also by others[62−64] for Pt, Ir, Ru, and Rh supported on various acidic supports. Moreover, Arribas et al.[65] demonstrated that the concentration and strength of the acid sites in Pt-modified USY zeolites were very similar to those of unmodified USY when most of the Pt crystallites were located at the external surface, i.e., not interacting with the acid sites inside the USY pores and cavities. It can therefore be suggested that the alteration of the electronic properties, which pertains to the metal at the interface with the support, also concerns the support. This results, then, in changes of the adsorption strength of pyridine on BAS as well as LAS and is witnessed as the redstribution of the acid site strengths in zeolites after their metal modification. An interpretation of this phenomenon from the point of view of the models suggested for metal−support interactions is discussed in more detail in section 3.3.

The changes in the distribution of acid site strengths (see Table 3) implicate the location of the Pt crystallites as well. The average crystallite size of Pt in MCM-41, 1.6 nm, is less than the diameter of the MCM-41 pores (ca. 3 nm), so it can be concluded that Pt is inside the pores of MCM-41 and therefore in contact with its acid sites. The conclusion is further supported by the observed changes in the distribution of acid site strengths (see Table 3) due to interactions between Pt crystallites and acid sites. On the other hand, the average sizes of Pt crystallites in zeolites (2.0−2.5 nm) exceed the diameter of the zeolite channels (ca. 0.8 nm), suggesting that, at least partially, the crystallites might be located at the external surface. However, the changes in the binding energy of Pt and in the linear adsorption band of CO (see Table 2), together with the altered distribution of the acid site strengths (see Table 3), are a sign of the interactions between the acid sites and the Pt crystallites. The acid sites are predominantly present at the internal surface,[66] and to explain their interactions with Pt crystallites, it is inferred that a portion of the Pt crystallites is located in the pores as well. Accordingly, no changes in the distribution of acid site strengths were observed in Pt/USY containing large Pt crystallites (>8 nm) predominantly at the external surface.[65] Moreover, these crystallites must consist of only a few atoms each, because the total concentration of the acid sites does not decrease significantly after impregnation (see Table 3), which means that the crystallites do not prevent pyridine adsorption on the acid sites, i.e., they do not block the pores. In addition, larger crystallites might be present in the zeolite channels than expected from the zeolite pore size if they form only "raft-like" particles[15] or are located at pore intersections. Moreover, the introduction of Pt did not cause any visible changes in the XRD patterns of the zeolites, suggesting that their structure was not severely damaged because of the formation of large Pt crystallites.

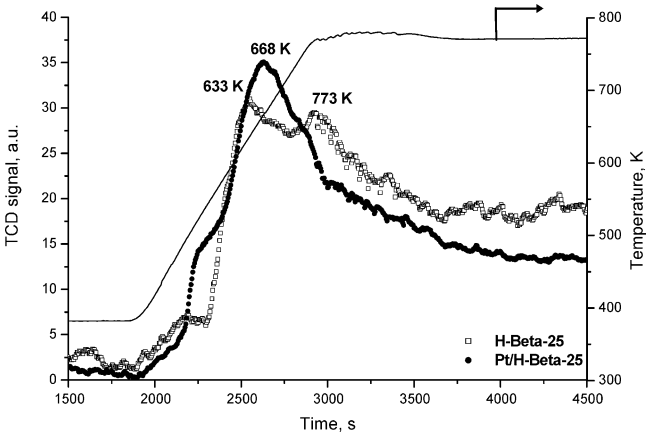

Figure 4. NH_3 TPD profiles of Pt/H−Beta-25 (filled symbols) and H−Beta-25 (open symbols).

The acidic properties of H−Beta-25 and Pt/H−Beta-25 were further investigated using the temperature-programmed desorption of ammonia (NH_3 TPD). Although just a minor decrease in the total acidity (from 740 to 660 μmol/g) could be found after the impregnation of H−Beta-25, a more profound change can be observed in the respective NH_3 desorption profiles (see Figure 4). In the case of H−Beta-25, two desorption maxima, at 633 and 773 K, can be distinguished, whereas only one maximum, at 668 K, can be found for Pt/H−Beta-25. It is well-known that the broadening of desorption peaks is attributable to the increasing heterogeneity of adsorption centers[67−69] and that the higher desorption temperature can be interpreted as the higher strength of such centers.[68,69] Accordingly, it can be concluded, on the basis of an analysis of the NH_3 desorption profiles (see Figure 4), that H−Beta-25 contains stronger acid sites (Brønsted and Lewis acid sites) than Pt/H−Beta-25, i.e., that the strength of the acid sites in H−Beta-25 was reduced as a result of its impregnation with Pt, which concurs with the conclusions based on pyridine adsorption/desorption.

3.2.2. Evidence from the Model Reaction: Conversion of Decalin. The reaction of decalin on proton-form and platinum-modified zeolites provides further evidence of the modification of the strength of acid sites in zeolites. As was shown recently,[34] decalin is transformed into a mixture of its skeletal isomers; ring-opening products (ROPs), i.e., C_{10} alkylcyclohexanes and C_{10} alkylcyclopentanes; and cracking products (CPs), i.e., hydrocarbons having less than 10 carbon atoms in molecule, on acidic zeolites. The transformation of decalin on zeolites is of consecutive nature;[34,35] isomers are the primary products and are converted in the course of reaction further into ROPs, which ultimately yield CPs (see Figure 5). When zeolites are modified with platinum, the conversion of decalin follows the same overall reaction scheme (see Figure 5), but the initial reaction step of the underlying reaction mechanism is different. Whereas protolytic cracking has been proposed as the initial reaction step on proton-form zeolites[34] to explain their activity, a bifunctional mechanism involving decalin dehydrogenation on metal sites followed by the protonation of the intermediate olefins on

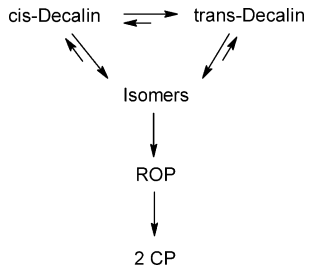

Figure 5. Simplified reaction scheme.

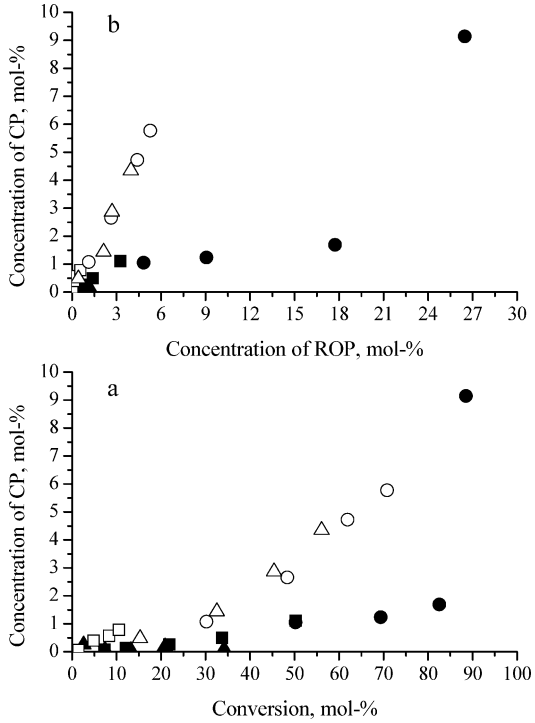

Figure 6. Dependence of the concentration of cracking products (CPs) on (a) the conversion of decalin and (b) the concentration of ring-opening products (ROPs) on proton-form (open symbols) and platinum-modified (filled symbols) zeolites. Catalysts: H− and Pt/H−Mordenite (□, ■), H− and Pt/H−Beta-25 (○, ●), H− and Pt/H−Beta-75 (△, ▲).

Brønsted acid sites has been put forward to account for the increase in zeolite activity upon impregnation with platinum.[35,65] The activity of Pt/H−MCM-41 was very low, with virtually no formation of ring-opening and cracking products, manifesting once again the bifunctional nature of the reaction and the need for Brønsted acid sites to accomplish decalin isomerization and ring opening. Because the reaction is affected by the presence of platinum, careful analysis of the reaction data is essential to elucidate the contribution of the individual active sites, i.e., metal sites and acid sites, to the observed overall performance of platinum-modified zeolites.

The differences in the formation of the cracking products (CPs) on the proton-form zeolites, on one hand, and the platinum-modified zeolites, on the other hand, reveal a change in the intrinsic activity of the active sites responsible for cracking (see Figure 6). In the case of proton-form zeolites, the cracking activity is attributable solely to the acid sites present in these zeolites, i.e., predominantly to the Brønsted acid sites.[34] The platinum-modified zeolites contain the same acid sites, and as shown by FTIR measurements (see Table 3), their total concentration even increases after impregnation with platinum. Hence, it could be expected that they would exhibit the same cracking activity as proton-form zeolites or even higher, if hydrogenolysis on Pt sites were involved. However, the formation of CPs is suppressed on zeolites containing platinum. This indicates that the cracking activity of zeolites does not correlate with the total acidity of the investigated zeolites and that platinum-catalyzed hydrogenolysis does not contribute substantially to the formation of CPs. Moreover, the platinum-modified zeolites were prepared by impregnation of their corresponding proton-form counterparts, and thus, the observed changes in product distribution cannot be attributed to the differences in zeolite structure or crystallite size. In theory, the inaccessibility of the acid sites to decalin after zeolite impregnation with Pt and their concurrent accessibility to pyridine could explain the decrease in the cracking activity of platinum-modified zeolites. However, the acid sites were demonstrated to be essential for the isomerization of decalin,[34,35] and because the rate of this reaction is augmented by the introduction of platinum,[35] it can be inferred that the acid sites are accessible to decalin and thus are not blocked by platinum clusters. Having excluded the other properties as irrelevant to the decrease of the cracking product formation on Pt-modified zeolites, the change in the distribution of the acid site strengths remains the only plausible property that could influence the cracking activity of the zeolites.

An examination of the reaction data (see Figure 6) and the distribution of the acid site strengths (see Table 3) reveals that they are in good agreement with the proposed explanation, i.e., that the strongest acid sites are the most important active sites for the cracking reactions. The comparison of proton-form zeolites shows that the same amounts of cracking products (CPs) are formed on H−Beta-25 and H−Beta-75 at similar conversions (see Figure 6a) and that H−Mordenite yields more CPs at low conversions than Beta zeolites. This concurs with the differences in the distribution of the acid site strengths (see Table 3): the concentrations of the strongest Brønsted acid sites (BAS) are similar for the two H−Beta zeolites, whereas this concentration is much higher in H−Mordenite. Moreover, none of the strongest acid sites are present in zeolites modified by platinum (see Table 3), and consequently, the Pt-modified zeolites exhibit lower cracking activities at comparable conversions than their corresponding H-form counterparts (see Figure 6). It can thus be concluded from the experimental data on decalin ring opening that the introduction of platinum into zeolites results in the reduction of the acid site strengths and, consequently, in the suppression of the cracking reactions. The sudden increase in the concentration of CPs at conversion levels above 80%, as seen in Figure 6, is due to the high concentration of ROPs, which are the only products in the reaction mixture forming CPs. The high concentration of ROPs originates from the suitable isomers formed in consecutive isomerization steps from decalin.[34,35] Similar dependences demonstrating sharp changes in selectivity within a narrow range of conversions are typical for many consecutive reactions with substantial differences in apparent rate constants of reaction steps.

The relative distribution of cracking products (CPs) provides yet another piece of evidence for the changes in the distribution of acid sites originating from the introduction of Pt into zeolites (see Table 4). It can be anticipated that a variation in the strength distribution of acid sites will affect not only the extent of cracking reactions, as discussed above, but also the relative abundances of different cracking products, as each of the cracking reactions requires acid sites of a different minimum strength. In other words, as the relative strength of the acid sites increases, the relative concentration of CPs originating from more demanding cracking reactions will increase as well. Because cracking reactions are undesirable in the ring opening of decalin and therefore their extent has to be minimized, just

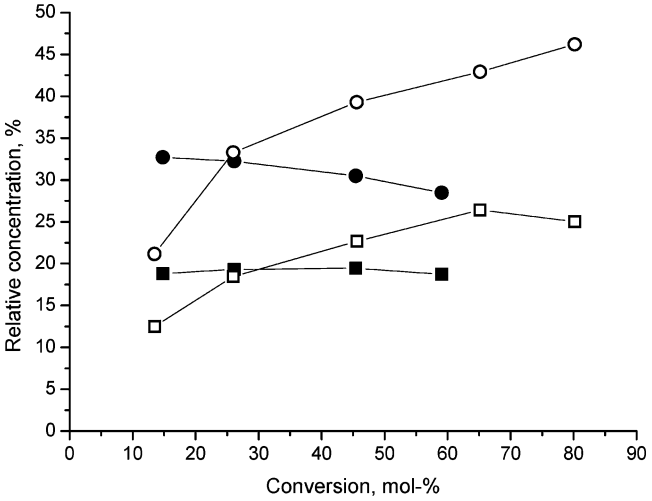

Figure 7. Relative concentration of C_4 (■, □) and C_6 (●, ○) hydrocarbons in the cracking products as a function of conversion on H−Beta-25 (filled symbols) and Pt/H−Beta-25 (open symbols).

TABLE 4: Relative Composition of Cracking Products on H−Beta-25 and Pt/H−Beta-25

	H−Beta-25		Pt/H−Beta-25	
conversion, %	26.1	45.4	26.0	45.6
cracking products, mol %	1.05	2.32	0.23	0.56
Relative Composition, %				
C_3	2.0	2.0	3.0	2.8
C_4	19.3	19.5	18.5	22.7
C_5	4.8	5.1	4.8	2.9
C_6	32.2	30.5	33.3	39.3
C_7	23.0	23.9	6.8	12.0
C_8	13.6	13.0	15.4	9.5
C_9	4.8	5.4	18.3	10.9

small concentrations of CPs (<5%) are obtained in the final product mixture. Consequently, a detailed quantitative analysis of cracking products is limited. Nevertheless, it is still possible to evaluate the differences in the composition of CPs in a qualitative manner. For this purpose, the CPs were grouped according to the number of carbons in the molecule (see Table 4). The data presented in Table 4 show that the formation of C_7 hydrocarbons is preferred on H−Beta-25 at the expense of C_4 and C_6 hydrocarbons at a comparable conversion level. The comparison of the relative concentrations of C_4 and C_6 on H−Beta-25, on one hand, and on Pt/H−Beta-25, on the other hand, as a function of conversion, which is presented in Figure 7, reveals an opposite trend of the relative concentration of the most abundant products: whereas there is a slight decline in the relative concentrations of C_4 and C_6 hydrocarbons with increasing conversion on H−Beta-25, the relative concentration of these CPs increases on Pt/H−Beta-25. To explain the observed distribution of the cracking products, one has to understand the peculiarities of the hydrocracking of naphthenes.[70,71] It was shown experimentally[70] and supported theoretically[71] that cracking of the internal bonds in naphthenes (endocyclic cracking) is unfavorable and that the elimination of the side chains on a naphthenic species is preferred where possible. Moreover, Egan et al. demonstrated[70] that a rearrangement of the side chains precedes their cleavage, i.e., that the side chains in tetramethylcyclohexane, for example, will be rearranged in such a way as to produce cyclohexane/methylcyclopentane and isobutane as the exclusive cracking products. Because ring-opening products, which undergo cracking in the present study, are C_{10} naphthenes as well, it is reasonable to expect that the same rules will apply for their cracking as mentioned above. In such a case, C_4 (isobutane) and C_6 (cyclohexane and methylcyclopentane) hydrocarbons are expected to be the predominant cracking products. Indeed, they represent between ca. 50% and 70% of all cracking products. Furthermore, it can be anticipated that the less favored cracking pathways (i.e., the more energetically demanding ones) will require stronger acid sites to be accomplished, which, in fact, can be observed here given that such products are more abundant on H−Beta-25 than on Pt/H−Beta-25 (see Table 4, Figure 7). This is consistent with the findings concerning the extent of cracking reactions on these two catalysts as well as with the acidity measurements by means of pyridine adsorption followed by FTIR spectroscopy and NH_3 TPD. All of these results lead to the same conclusion that the strength of the acid sites in zeolites is decreased through the introduction of platinum into them.

3.3. Implications from Models Describing Metal−Support Interactions. The models describing the metal−support interactions in zeolites focus only on the influence of the support on the properties of the supported metal crystallites,[3,20,24−27,29] and because none of the experimental data on which these models are based describe the support properties, the models obviously cannot be used to describe the influence of the metal crystallites on the support. However, as the alteration of the support properties, namely, of the support acidity, has been now established, it is of vital importance to compare the current observations with the previous results and determine whether the models can be extended to include the mutuality of the metal−support interactions. This analysis is aimed at the most recent model, the interatomic potential model,[20] which seems to describe the metal−support interactions most coherently among all of the models suggested.

The primary interaction in the interatomic potential model is a Coulomb attraction between the metal crystallites and the support oxygen ions.[20] The support interaction consequently leads to a change in the interatomic potential of the metal valence orbitals,[20] which is caused by an alteration of in the electron charge of the support oxygen atoms.[29] The composition of the support determines the Madelung potential of the support and, hence, the electron charge of the support oxygen atoms.[29] It is thus conceivable that a modification of the support, e.g., by impregnation of the support with a metal, will unavoidably lead to changes in the Madelung potential of the support. Such changes will, in turn, affect the electron charge of the support oxygen atoms and ultimately modify the interatomic potential of the metal valence orbitals. Once the electron charge of the support oxygen atoms is altered, it is plausible to expect that the strength of the proton−oxygen bond of the bridging hydroxyl groups will be altered as well, i.e., the willingness to donate a proton to adsorbing molecules (the Brønsted acidity) will change. For example, in accordance with the model, the metal−support interface is richer in electrons on an acidic support after the introduction of a metal, e.g., platinum, and because of the higher richness in electrons at the interface, i.e., at the support oxygen atoms, the hydrogen−oxygen bonds of the bridging hydroxyl groups becomes less ionic, i.e., their acidity is decreased. A molecular orbital scheme, proposed by Ramaker et al.[29] for the interaction between an interfacial Pt atom and a support oxygen atom, helps to further clarify the impact of supported Pt on the acidity of the support. The direct electronic interaction between the Pt 6s interstitial bonding orbital and the O $2p_z$ orbitals results, in the case of an acidic support, in the lowest molecular orbital being closer to the metal−support interface, i.e., in a net charge movement from the Pt cluster to

the metal−support interface.[29] As a consequence, the O−H bond will become shorter because of a larger overlap between the corresponding O and H orbitals, i.e., the acidity of such protons will decrease. Because the change in acidity has now been observed experimentally, it can be suggested that the interatomic potential model is capable of explaining not only the changes of the metal properties,[20,27,29] but also the changes in the support acidity. Nevertheless, theoretical calculations would be useful to further support this theory.

4. Conclusions

Metal−support interactions have been investigated by means of XPS, CO and pyridine adsorption, H_2 and NH_3 TPD, and a model reaction (ring opening of decalin) on a series of platinum-modified catalysts of different acidities. The results clearly show that the interactions between the platinum and the support are mutual, i.e., that the support affects the properties of the platinum and that, at the same time, the properties of the support are influenced by the platinum. The changes in the electronic properties of the supported platinum crystallites are evidenced by the shifts of the Pt binding energy in XPS and of the stretching frequency of linearly adsorbed CO. The changes depend on the catalyst acidities: the shifts are increased with increasing concentration of the acid sites. At the same time, the acidic properties of the supports are affected by platinum, as indicated by the redistribution of the acid site strengths and the changes in the product selectivities in the ring opening of decalin. When the zeolites and H−MCM-41 are impregnated with Pt, the strength of their acid sites is significantly reduced: virtually none of the strongest acid sites are present in the Pt-modified catalysts. The extent of the cracking reactions is suppressed, and the cracking selectivity is altered in the Pt-modified catalysts, which can be explained by the reduced strength of the acid sites as well.

The interatomic potential model,[20] proposed to describe metal−support interactions, was examined in this study to determine whether it can be used to account for the changes in the support acidity due to the metal. It was found that the changes in the interatomic potential and the induced charge rearrangement from the particle to or from the metal−support interface[29] can explain the observed redistribution of the acid site strengths. Furthermore, the acidity measurements indicate that collective interactions are involved in the metal−support interactions.

Acknowledgment. This work is part of the activities at Åbo Akademi Process Chemistry Centre within the Finnish Centre of Excellence Programme (2000-2005) by the Academy of Finland. The authors express their gratitude to Teemu Heikkilä (University of Turku) for the XRD characterization of the catalysts. Economic support from Neste Oil and TEKES is gratefully acknowledged.

References and Notes

(1) Gates, B. C. *Chem. Rev.* **1995**, *95*, 511.
(2) Gates, B. C. In *Preparation of Solid Catalysts*; Ertl, G., Knözinger, H., Weitkamp, J., Eds.; Wiley-VCH: New York, 2001; p 371.
(3) Sachtler, W. M. H.; Zhang, Z. *Adv. Catal.* **1993**, *39*, 129.
(4) Sachtler, W. M. H. In *Preparation of Solid Catalysts*; Ertl, G., Knözinger, H., Weitkamp, J., Eds.; Wiley-VCH: New York, 2001; p 388.
(5) Sachtler, W. M. H. *Acc. Chem. Res.* **1993**, *26*, 383.
(6) Gault, F. *Adv. Catal.* **1981**, *30*, 1.
(7) Alvarez, W. E.; Resasco, D. E. *Catal. Lett.* **1991**, *8*, 53.
(8) Gallezot, P.; Giroir-Fendler, A.; Richrd, D. *Catal. Lett.* **1990**, *5*, 169.
(9) Martens, J. A.; Tielen, M.; Jacobs, P. A. *Catal. Today* **1987**, *1*, 435.
(10) Martens, J. A.; Jacobs, P. A.; Weitkamp, J. *Appl. Catal.* **1986**, *20*, 239.
(11) Weitkamp, J. *Ind. Eng. Chem. Prod. Res. Dev.* **1982**, *21*, 550.
(12) Magnoux, P.; Cartraud, P.; Mignard, S.; Guisnet, M. *J. Catal.* **1987**, *106*, 235.
(13) Magnoux, P.; Cartraud, P.; Mignard, S.; Guisnet, M. *J. Catal.* **1987**, *106*, 242.
(14) Dalla Betta, R. A.; Boudart, M. In *Proceedings of the 5th International Congress on Catalysis*; Hightower, H., Ed.; North Holland: Amsterdam, 1973; p 1329.
(15) Stakheev, A. Yu.; Kustov, L. M. *Appl. Catal. A: Gen.* **1999**, *188*, 3.
(16) de Mallmann, A.; Barthoumeuf, D. *J. Chem. Phys.* **1990**, *87*, 535.
(17) Primet, M. *J. Catal.* **1984**, *88* (2), 273.
(18) Primet, M.; De Menorval, L. C.; Fraissard, J.; Ito, T. *J. Chem. Soc., Faraday Trans.* **1985**, *81* (11), 2867.
(19) Tri, T. M.; Candy, J. P.; Gallezot, P.; Massardier, J.; Primet, M.; Vedrine, J. C.; Imelik, B. *J. Catal.* **1983**, *79*, 396.
(20) Mojet, B. L.; Miller, J. T.; Ramaker, D. E.; Koningsberger, D. C. *J. Catal.* **1999**, *186*, 373.
(21) Koningsberger, D. C.; Ramaker, D. E.; Miller, J. T.; De Graaf, J.; Mojet, B. L. *Top. Catal.* **2001**, *15*, 35.
(22) Stakheev, A. Yu.; Sachtler, W. M. H. *J. Chem. Soc., Faraday. Trans.* **1991**, *87*, 3703.
(23) Blackmond, D. G.; Goodwin, J. G., Jr. *J. Chem. Soc., Chem. Commun.* **1981**, 125.
(24) Homeyer, S. T.; Karpinski, Z.; Sachtler, W. M. H. *J. Catal.* **1990**, *123*, 60.
(25) Sachtler, W. M. H.; Stakheev, A. Yu. *Catal. Today* **1992**, *12*, 283.
(26) Jansen, A. P.; van Santen, R. A. *J. Phys. Chem.* **1990**, *94*, 6764.
(27) Koningsberger, D. C.; De Graaf, J.; Mojet, B. L.; Ramaker, D. E.; Miller, J. T. *Appl. Catal. A: Gen.* **2000**, *191*, 205.
(28) Miller, J. T.; Mojet, B. L.; Ramaker, D. E.; Koningsberger, D. C. *Catal. Today* **2000**, *62*, 101.
(29) Ramaker, D. E.; De Graaf, J.; Van Veen, J. A: R.; Koningsberger, D. C. *J. Catal.* **2001**, *203*, 7.
(30) Vaarkamp, M.; Miller, J. T.; Modica, F. C.; Koningsberger, D. C. *J. Catal.* **1996**, *163*, 294.
(31) Kustov, L. M.; Vasina, T. V.; Ivanov, A. V.; Masloboishchikova, O. V.; Khelkovskaya-Sergeeva, E. V.; Zeuthen, P. *Stud. Surf. Sci. Catal.* **1996**, *101*, 821.
(32) Valyon, J.; Engelhardt, J.; Lónyi, F.; Kalló, D.; Gömöry, Á. *Appl. Catal. A: Gen.* **2002**, *229*, 135.
(33) Aboul-Gheit, A. K.; Aboul-Fotouh, S. M.; Aboul-Gheit, N. K. *Appl. Catal. A: Gen.* **2005**, *292*, 144.
(34) Kubička, D.; Kumar, N.; Mäki-Arvela, P.; Tiitta, M.; Niemi, V.; Salmi, T.; Murzin, D. Yu. *J. Catal.* **2004**, *222*, 65.
(35) Kubička, D.; Kumar, N.; Mäki-Arvela, P.; Tiitta, M.; Niemi, V.; Karhu, H.; Salmi, T.; Murzin, D. Yu. *J. Catal.* **2004**, *227*, 313.
(36) Beck, J. S.; Vartuli, J. C.; Roth, W. J.; Leonowicz, M. E.; Kresge, C. T.; Schmitt, K. D.; Chu, C. T. W.; Olson, D. H.; Sheppard, E. W.; McCullen, S. B.; Higgins, J. B.; Schlenker, J. L. *J. Am. Chem. Soc.* **1992**, *114*, 10834.
(37) Reddy, K. M.; Song, C. *Catal. Lett.* **1996**, *36*, 103.
(38) Kumar, N.; Mäki-Arvela, P.; Hájek, J.; Salmi, T.; Murzin, D. Yu.; Heikkilä, T.; Laine, E.; Laukkanen, P.; Väyrynen, J. *Microporous Mesoporous Mater.* **2004**, *69*, 173.
(39) (a) Anderson, J. R. *Structure of Metallic Catalysts*; Academic Press: New York, 1975. (b) Kalantar Neyestanaki, A.; Klingstedt, F.; Salmi, T.; Murzin, D. Yu. *Fuel* **2004**, *83*, 395. (c) Lieske, H.; Lietz, G.; Spindler, H.; Völter, J. *J. Catal.* **1983**, *81*, 8.
(40) Zeolyst International, www.zeolyst.com (accessed Oct 2005).
(41) Marques, J. P.; Gener, I.; Ayrault, P.; Bordado, J. C.; Lopes, J. M.; Ribeiro, F. R.; Guisnet, M. *C. R. Chim.* **2005**, *8*, 399.
(42) Moulder, J. F.; Stickle, W. F.; Sobol, P. E.; Bomben, K. D. *Handbook of X-ray Photoelectron Spectroscopy*; Physical Electronics Division, Perkin-Elmer Corp.; Wellesley, MA, 1992.
(43) Emeis, C. A. *J. Catal.* **1993**, *141*, 347.
(44) Haller, G. L.; Resasco, D. E. *Adv. Catal.* **1989**, *36*, 173.
(45) Hayek, K.; Kramer, R.; Paál, Z. *Appl. Catal. A: Gen.* **1997**, *162*, 1.
(46) Fung, S. C. *J. Catal.* **1982**, *76*, 225.
(47) Larsen, G.; Haller, G. L. *Catal. Lett.* **1989**, *3*, 103.
(48) Zeolyst International, www.zeolyst.com.
(49) Marks, F. A.; Lindau, I.; Browning, R. *J. Vac. Sci. Technol. A* **1990**, *8*, 3437.
(50) Nosova, L. V.; Stenin, M. V.; Nogin, Yu. N.; Ryndin, Yu. A. *Appl. Surf. Sci.* **1992**, *55*, 43.
(51) de Ménorval, L.-C.; Chaqroune, A.; Coq, B.; Figueras, F. *J. Chem. Soc., Faraday Trans.* **1997**, *93*, 3715.
(52) Stoop, F.; Toolenaar, F. J. C. M.; Ponec, V. *J. Catal.* **1982**, *73*, 50.

(53) Blyholder, G. *J. Phys. Chem.* **1964**, *68*, 2772.
(54) Miller, J. T.; Meyers, B. L.; Barr, M. K.; Modica, F. S.; Koningsberger, D. C. *J. Catal.* **1996**, *159*, 41.
(55) Miller, J. T.; Meyers, B. L.; Modica, F. S.; Lane, G. S.; Vaarkamp, M.; Koningsberger, D. C. *J. Catal.* **1993**, *143*, 395.
(56) Savchits, M. F.; Ustilovskaya, Eh. Ya.; Veshtert, V. Z.; Agabekova, L. A.; Egiazarov, Yu. G. In *Proceedings of the 10th International Congress on Catalysis, 1992*; Guczi, L., Solymosi, F., Tetenyi, P., Eds.; Elsevier Science Publishers B. V.: Budapest, Hungary, 1993; p 1645.
(57) Nieminen, V.; Kumar, N.; Datka, J.; Päivärinta, J.; Hotokka, M.; Laine, E.; Salmi, T.; Murzin, D. Yu. *Microporous Mesoporous Mater.* **2003**, *60*, 159.
(58) Auroux, A.; Gervasini, A.; Guimon, C. *J. Phys. Chem. B* **1999**, *103*, 7195.
(59) Beyer, H. K. Dealumination Techniques for Zeolites. In *Postsynthesis Modification I, Molecular Sieves Science and Technology*; Karge, H. G., Weitkamp, J., Eds.; Springer: Berlin, 2002; Vol. 3, pp 204−255.
(60) Marques, J. P.; Gener, I.; Ayrault, P.; Lopes, J. M.; Ramoa Ribeiro, F.; Guisnet, M. *Chem. Commun.* **2004**, *20*, 2290.
(61) Vijayalakshmi, R.; Kapoor, S.; Kulshreshtha, S. K. *Solid State Sci.* **2002**, *4*, 489.
(62) Nieminen, V. Doctoral Thesis, Åbo Akademi University, Åbo, Norway, 2004.
(63) Nieminen, V.; Kangas, M.; Salmi, T.; Murzin, D. Yu. *Ind. Eng. Chem. Res.* **2005**, *44*, 471.
(64) Løften, T. Doctoral Thesis, Norwegian University of Science and Technology, Trondheim, Norway, 2004.
(65) Arribas, M. A.; Concepción, P.; Martínez, A. *Appl. Catal. A: Gen.* **2004**, *267*, 111.
(66) Jansen, J. C.; Creyghton, E. J.; Njo, S. L.; van Konigsveld, H.; van Bekkum, H. *Catal. Today* **1997**, *38*, 205.
(67) Tovbin, Yu. K.; Votyakov, E. V. *Langmuir* **1999**, *15*, 6070.
(68) Karge, H. G.; Dondur, V. *J. Phys. Chem.* **1991**, *95*, 283.
(69) Karge, H. G.; Dondur, V.; Weitkamp, J. *J. Phys. Chem.* **1990**, *94*, 765.
(70) Egan, C. J.; Langlois, G. E.; White, R. J. *J. Am. Chem. Soc.* **1962**, *84*, 1204.
(71) Weitkamp, J.; Ernst, S. *Catal. Today* **1994**, *19*, 107.